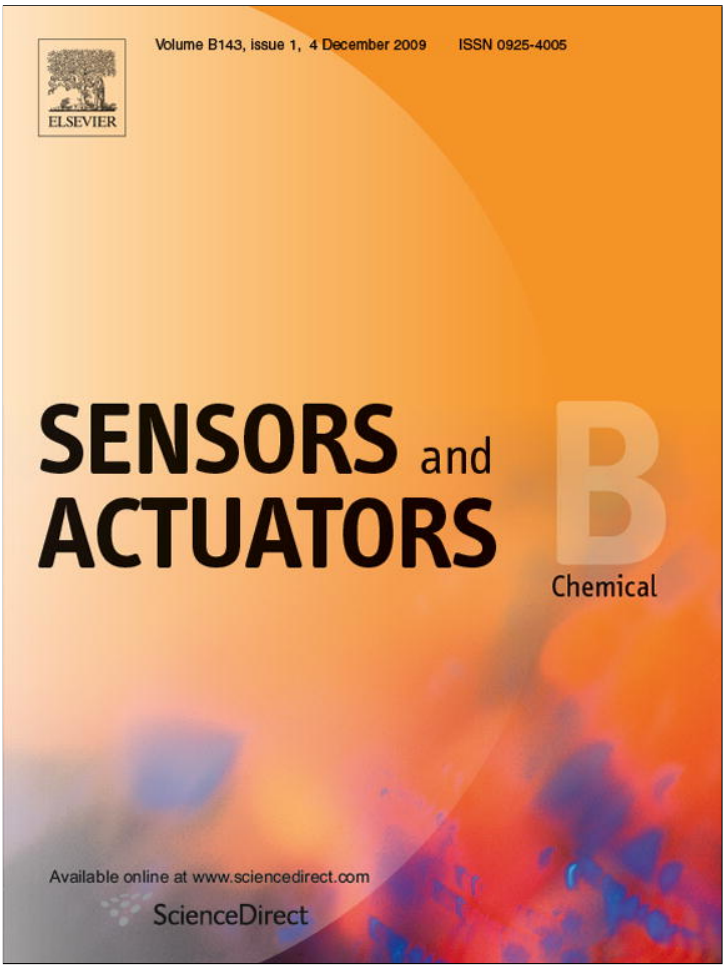

Sensors and Actuators B 143 (2009) 286–294

Contents lists available at ScienceDirect

Sensors and Actuators B: Chemical

journal homepage: www.elsevier.com/locate/snb

Theoretical and experimental investigation of spatial temperature gradient effects on cells using a microfabricated microheater platform

Ankur Jain*, Kevin Ness[1], Kenneth E. Goodson

Microscale Heat Transfer Laboratory, Department of Mechanical Engineering, Stanford University, Stanford, CA 94305, USA

ARTICLE INFO

Article history:
Received 1 June 2009
Received in revised form 12 August 2009
Accepted 15 August 2009
Available online 25 August 2009

Keywords:
Bio-MEMS
Thermal sensor
Thin film microheater
Thermotaxis

ABSTRACT

While the cellular interaction with the chemical microenvironment has been studied in detail in the past, the effect of thermal signals and gradients on cells is not well understood. While almost all biological macrosystems exhibit temperature sensitivity, this has not been studied much at the cellular level. The capability of precise control of temperature and heat flux at the scale of a few microns using microfabricated structures makes microelectromechanical systems (MEMS) ideal for investigating these effects. This work describes a MEMS-based microheater platform capable of subjecting surface-adhered cells to microscale temperature gradients. This microdevice comprises a free-standing thin film based microheater platform. The design and microfabrication of this microdevice are described. A thermal conduction model is developed in order to thermally characterize the microheater platform. Protocols for culturing cells on the microheater platform are developed, making it possible to adhere cells on the microheater surface and subject them to a desired spatial temperature gradient. Experiments demonstrating the spatial control of cell viability using the microheater device are described. This is followed by experiments that explore the possibility of cellular growth in response to thermal gradients, similar to chemotaxis. Thermotactic effect is well known at the organismal level. However, cells used in this work did not exhibit any thermotactic effect. A theoretical model for predicting cell response to a spatial temperature gradient in its microenvironment is proposed. The model is based on the effect of the temperature gradient on the chemical sensory process of the cell. The model predicts that in addition to the thermal gradient, the thermotactic effect also depends on a number of other parameters that have not been well characterized in the past. The microheater platform described in this work offers a fundamental new experimental tool with which to explore the interaction of cellular systems with their thermal microenvironment. The theoretical model of thermotaxis developed here furthers the understanding of the function of a cell as a thermal and chemical sensor.

1. Introduction

The past few decades have witnessed increased interest in applying analytical and experimental methods of engineering nature to problems in biology and medicine. Advances in microelectromechanical systems (MEMS) and microfluidics have enabled the development of tools that can investigate and manipulate biological microsystems like cells, proteins and DNA [1–3]. While on one hand, this has led to an improved fundamental understanding of cellular phenomena, a practical application has been the miniaturization of a variety of bioanalytical tools and assays [3]. In the recent past, MEMS-based PCR devices have achieved excellent temperature control [4], leading to improved cycling rates and decreased sample volume requirements [5]. Temperature Gradient Focusing (TGF) in a microchannel offers significant improvement in several separation and concentration assays [6]. MEMS devices have also been used for achieving temperature uniformity in a DNA detection chip to enable hybridization in a small temperature range [7]. The capability of manipulation at small spatial scales offered by MEMS makes it possible to study the cellular interaction with its physical and chemical microenvironments [8]. This interaction is fundamental to understanding the behavior of biological microsystems, including cellular locomotion, growth, viability, etc. In contrast to physical and chemical factors such as surface topology, electric field, chemical species, etc., cellular response to thermal signals has not been studied in much detail, except for experiments in isothermal conditions [9,10]. While most thermal-based devices rely on temperature uniformity, the use of temperature gradients in time or space for manipulation and diagnostics has received very little attention. One possible reason for the lack of interest in this direction is that temperature gradients are not as common *in vivo* as chemical gradients. Temperature Gradient Gel Electrophoresis

* Corresponding author. Current address: Molecular Imprints Inc., Austin, TX 78613, USA. Tel.: +1 512 419 8327; fax: +1 650 723 3521.
E-mail address: ankurjain@stanfordalumni.org (A. Jain).
[1] Current address: Quanta Life, Inc., Livermore, CA, USA.

0925-4005/$ – see front matter © 2009 Elsevier B.V. All rights reserved.
doi:10.1016/j.snb.2009.08.035

(TGGE) uses the composition dependence of the DNA melting temperature to separate strands based on the relative concentrations of A–T and G–C bonds, which have differing strengths [11]. Spatial temperature gradients have been used for focusing and separation in microfluidic devices [6]. These applications indicate the importance of temperature gradients for control of reactions and separation, but clearly much more research needs to be performed on other applications, especially the investigation of living cells. While the well known temperature sensitivity of organisms [12,13] may serve as a good physiological motivation behind such a study, a possible reason for the lack of work on temperature gradients is the difficulty of interfacing precise temperature control with single, live cells using traditional experimental tools. This capability is available in MEMS-based microstructures, making it possible to examine thermal effects at the cellular level. Thin film membrane based microstructures are particularly attractive due to the possibility of accurate thermal control and quick response time [14].

The response of a cell or an organism to an imposed spatial temperature gradient is referred to as thermotaxis. While the temperature sensitivity of organisms is well known, there is a lack of biophysical models for predicting the influence of temperature fields in the cellular microenvironment on the cell behavior. Temperature fluctuation around a cell has been treated at best as a noise in the cellular sensory process, and the effect of this noise on the search for food has been theoretically investigated [15]. Some work has been performed on experimentally studying thermotaxis at the organismal level. For example, when subjected to a spatial temperature gradient, *C. elegans* nematodes have been observed to migrate to the temperature at which they were cultivated, and then closely follow isotherms in their motion paths [12,13]. Some work has been carried out in order to elucidate the cellular basis of such organismal behavior. Specific neurons responsible for organismal level thermotaxis in *C. elegans* have been identified through a systematic elimination method [16]. Yet, the direct interaction of isolated nerve cells with a thermal field has not been reported. At the molecular level, thermal sensing is believed to be associated with specific TRP ion channels [17,18].

This paper makes two contributions to the study of thermal effects in cells. Firstly, it describes a MEMS-based microheater platform capable of subjecting isolated, surface-adhered cells to spatial temperature fields. Secondly, it develops a theoretical model for understanding the cellular sensory response to a spatial temperature field. In the next section, the thermo-mechanical design and fabrication of the MEMS-based microheater device are discussed. Development of cell culturing protocols for adhering Pheochromocytoma (PC12) cells [19] and 3T3 fibroblast cells [20] on the surface of the microheater device is also discussed. Experiments on spatial control of cell lysing and thermotaxis are described. Section 3 discusses the theoretical modeling of thermal performance of the microheater device, and an equilibrium biochemistry-based theoretical model for understanding thermotactic effects in cells. Experimental and theoretical results are discussed in the following section.

2. Materials and methods

2.1. Design and microfabrication of the MEMS microheater platform

MEMS microfabrication technology offers the means to develop thermal control at the same scale as typical cells. A microheater platform capable of investigating thermal effects in cells requires three major components—a biocompatible surface suitable for cell culturing, a heater element, and a temperature sensor. A free-standing thin film membrane based design ensures quick response time. Further, the membrane provides thermal isolation, and hence good temperature control. Microfabricated membranes have been used in the past for other applications such as gas sensing [14]. Unlike these applications, where silicon, the primary membrane material provides temperature uniformity due to its high thermal conductivity, the microheater membrane in the present study must comprise a low thermal conductivity material in order to produce large temperature gradients on the membrane surface. The membrane thickness is governed by stability requirements. The membrane material must have sufficient residual tensile stress in order for the membrane to remain taut after release. Silicon nitride is an excellent material that satisfies all of the above requirements. Electric current passing through a metal wire causes Joule heating and hence temperature rises in the membrane. The metal wire is designed to be much thinner than the membrane dimensions in order to minimize heat conduction in the wire. Thin film metal-based resistance temperature sensors are also provided on the membrane in order to measure local temperature rise. In addition, simultaneous 4-wire voltage and current measurement enables the heater to be used as a temperature sensor as well.

Fig. 1(a) shows a SEM of the microheater device microfabricated at the Stanford Nanofabrication Facility (SNF). A 1.7 μm thick layer of silicon nitride is deposited on a single-crystal double-side polished ⟨1 0 0⟩ silicon wafer in an LPCVD furnace at 850 °C. 0.2 μm aluminum is sputtered, patterned and dry-etched to define a heater line bisecting the membrane and three sensor elements. The widths of the heater and sensor lines are 10 μm and 2 μm respectively. Heater and temperature sensors are passivated from the environment by depositing a 0.4 μm thick film of silicon dioxide in an LPCVD furnace at 400 °C. Another step of photolithography followed by wet-etch is performed in order to gain electrical access to metal contact pads connecting to the heater and sensor elements. Pad etch (a mixture of acetic acid and ammonium fluoride) is used because of the relatively low etch rate of aluminum in pad etch. Silicon nitride deposited on the backside of the wafers is stripped. Finally, the device membrane is formed by photolithography, front-to-backside alignment and Deep Reactive Ion Etch (DRIE) of the silicon substrate from the backside. The etched wafers are diced and the resulting devices are soaked in acetone for photoresist removal. The final device is approximately 10 mm × 10 mm in size and has a 0.9 mm × 1.8 mm sized rectangular membrane. The membrane, metal heaters and three temperature sensors are clearly seen in Fig. 1(a).

Thermal characterization of the microheater devices is performed in a vacuum chamber at low pressure (<30 mTorr). The microheater device is mounted on a temperature controlled platform. The electrical resistances of the heater and temperature sensors are first calibrated as functions of temperature. DC power is then supplied using a Keithley-200 current source, and the voltages across the heater and temperature sensors are measured using HP3458A multimeters.

2.2. Cell culturing on the MEMS microheater platform

Fig. 1(b) shows an image of the microheater device in its final biocompatible package in a leadless chip carrier (LCC). A 10 mm through-hole is drilled through the base of the LCC in order to facilitate imaging of the microheater surface. The device is first glued on the backside and placed in the center of the LCC. This is followed by wire-bonding of metal contact pads on the device to gold pads on the LCC. Soldered wires on the periphery of the LCC provide a convenient electrical interface. In order to create a package compatible with standard wet laboratory procedures, the LCC is glued inside a small Petri dish with slots to allow wires to come out. Finally, the

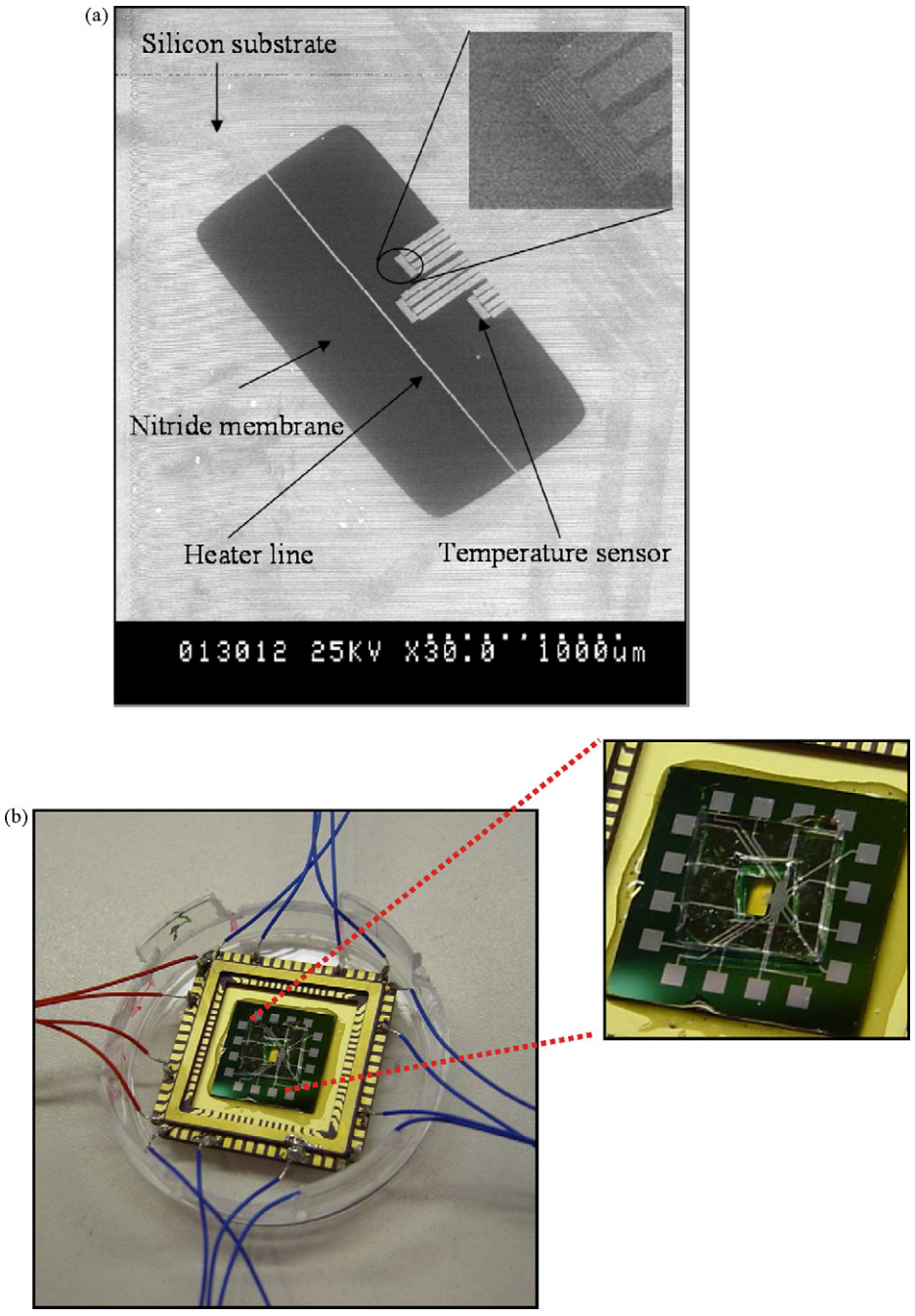

Fig. 1. (a) SEM of the microheater device and (b) image of the microheater device in the biocompatible package for cell culturing.

small Petri dish is glued on a larger Petri dish in order to control liquid spilling. A hollow gasket of polydimethylsiloxane (PDMS) is cut and carefully placed around the microheater membrane. This gasket prevents the cell culture media from contacting and eroding the metal contact pads. As an added precaution against contamination, PDMS is poured around the gasket and cured. As a result, all contact pads and wirebonds are effectively sealed off, leaving only the thin film membrane exposed.

Two types of cells – PC12 cells and 3T3 fibroblast cells – are used in the present study. The PDMS gasket around the microheater membrane is first filled with ethanol for about 5 min. The device is then rinsed with DI water 2–3 times. 3T3 cells are directly introduced on the microheater membrane in standard cell media. Cell adherence is observed within 20–30 min. Adherence of PC12 cells requires more complicated surface preparation using cell adhesion molecules. After cleaning with DI water, the membrane is treated with 0.1 mg/mL poly-lysine and 1 μL/mL solution laminin in neurobasal-A. PC12 cells in media are then introduced and the microdevice is incubated in a 5% CO_2 atmosphere at 37 °C for at least 4–5 h. Fig. 2 shows a typical fluorescent image of PC12 cells cultured on the microheater device. The metal heater line as well as a temperature sensor are seen in the background.

Both fluorescence and light microscopy are used for cell imaging. The thin film microheater membrane is transparent to visible light. A two-component live/dead cytotoxicity dye [21] is used for fluorescence imaging. One component of the dye penetrates the cell membrane of dead cells and fluoresces red by attaching to the cell nucleus. The other component of the dye attaches to the membrane of a live cell and fluoresces green. A three-color CCD camera

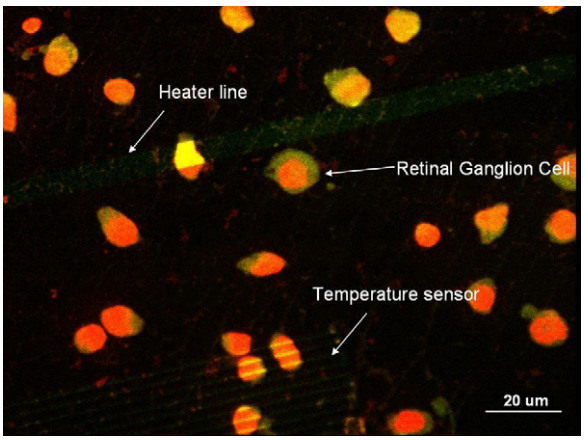

Fig. 2. Fluorescent image showing a typical culture of retinal ganglion cells obtained on the microheater device. Note the heater and temperature sensor in the background.

connected to a fluorescence microscope is used for imaging and distinguishing between live and dead cells.

3. Theory

3.1. Prediction of thermal performance of the microheater device

Accurate prediction of temperature rise in the microheater platform due to Joule heating in the metal wire requires the thermal conductivity of the membrane material. This parameter is used in finite element simulations for determining the temperature field on the microheater platform during experiments with cells. Since thermophysical properties of thin films are strongly dependent on size, temperature and processing history [22], an *in situ* measurement is preferred over handbook data. The thermal conductivity of the membrane is determined by comparing experimental data for temperature rise in vacuum as a function of heater power with predictions from an analytical heat transfer model. Consider a schematic of the microheater platform shown in Fig. 3. The narrow aluminum heater line bisecting the membrane produces Joule heating that is conducted through the membrane into the silicon substrate. Convective and radiative heat transfer paths are

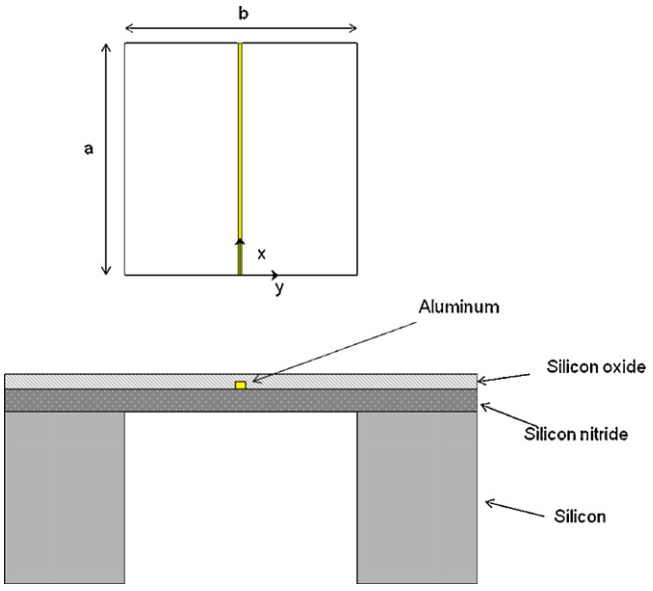

Fig. 3. Schematic of the geometry of the microheater platform.

negligible when the microheater platform is in vacuum, and the temperature rise is reasonably small [23]. The bulk silicon substrate is assumed to be isothermal due to its large thermal mass compared to the membrane [23]. Due to the small thickness of the membrane, temperature variation in the out-of-plane direction is neglected. Based on these assumptions, the governing equation for temperature is given by

$$k\left(\frac{d^2T}{dx^2}+\frac{d^2T}{dy^2}\right)=0 \tag{1}$$

where k is the thermal conductivity of the membrane.

The boundary conditions associated with Eq. (1) are

$$T(x=0,y)=T(x=a,y)=T\left(x,y=\frac{b}{2}\right)=T_0 \tag{2}$$

where T_0 is the ambient temperature.

Assuming that the heater line is much thinner than the membrane dimension, it may be modeled as a line source of heat. Considering only the right half of the membrane, this provides the following boundary condition

$$-k\left(\frac{dT}{dy}\right)_{y=0}=\frac{I^2R}{2at} \tag{3}$$

where t is the thickness of the membrane. I is the electric current passing through the heater line and R is the electrical resistance of the heater line.

An analytical solution for the temperature field on the microheater platform is found to be

$$T(x,y)=T_0+\sum_{n=1}^{\infty}\frac{I^2R(1-(-1)^n)}{(n\pi)^2tk\cosh(n\pi b/2a)}\sin\left(\frac{n\pi x}{a}\right)\times\sinh\left(\frac{n\pi}{a}\left(\frac{b}{2}-|y|\right)\right) \tag{4}$$

The average temperature rise in the heater line may be determined from Eq. (4) as follows:

$$T_{\text{avg,heater}}=T_0+\sum_{n=1}^{\infty}\frac{I^2R(1-(-1)^n)^2}{(n\pi)^3tk}\tanh\left(\frac{n\pi b}{2a}\right) \tag{5}$$

Comparison of Eq. (5) with experimental data enables the determination of the thermal conductivity of the membrane. Once this is done, the temperature profile on the membrane surface during experiments with cells is predicted using a finite element heat transfer model developed in ANSYS. The finite element model accounts for heat conduction within the membrane as well as into the liquid media containing cells. Thermal properties of water are used for modeling the cell media.

3.2. Biophysical model for thermotaxis

This section develops a quantitative model for understanding cellular interaction with a temperature field in its microenvironment and for predicting cellular level thermotaxis using the framework of ligand–receptor interactions. Ligand–receptor interactions have been widely studied in the context of cellular response to chemical gradients, known as chemotaxis. This involves the growth or migration of a cell towards higher concentration region of a chemical perceived to be useful for growth and survival, and vice versa. Chemotaxis is believed to be responsible for several *in vivo* processes including the creation of billions of neuronal connections in the developing embryo [24], nerve regeneration following injury in the peripheral nervous system [25] and the process of searching for food by unicellular organisms [15]. The chemical

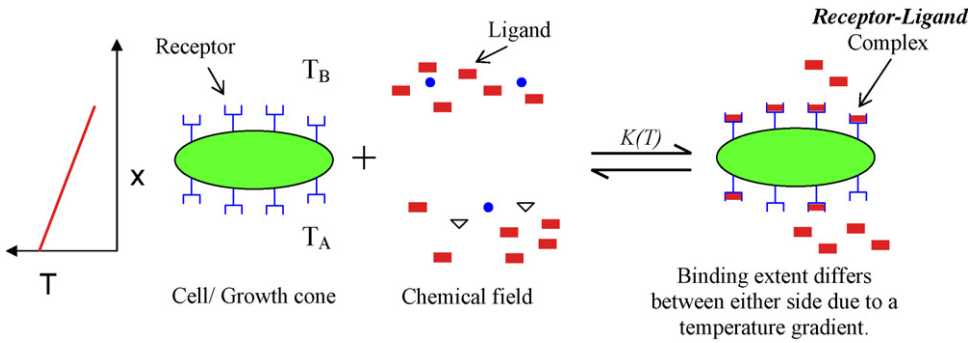

Fig. 4. Schematic of the ligand–receptor interactions in the presence of a temperature gradient. The temperature gradient influences the relative balance of the number of bound receptor sites on two sides of the cell. Note that the ligand of interest is shown as a red rectangle.

sensory process behind chemotaxis involves the binding of ligands in the cellular microenvironment to specific receptor sites on the cell membrane to form ligand–receptor complexes. A gradient in ligand concentration leads to a difference in the number of ligand–receptor complexes across the cell, which the cell is known to be capable of sensing [26,27]. When this difference exceeds a certain threshold, it triggers intra-cellular pathways, resulting in chemotactic response.

Consider Fig. 4 which shows a temperature gradient imposed across two faces A and B of a cell. Receptor sites corresponding to a specific ligand of are assumed to be distributed uniformly on the cell membrane. At equilibrium, the concentrations of ligand–receptor complexes and unbound ligands are governed by the equilibrium constant of the reaction. Let c be the ligand concentration in the cellular microenvironment and N_0 the total number of receptor sites on the cell membrane. Assuming uniform distribution of receptor sites, A and B both have $0.5N_0$ receptors each. Let the number of ligand–receptor complexes formed on each side of the cell be denoted as N_A and N_B. By neglecting second-order effects such as the presence of two different classes of receptor sites, each of which has different reaction dynamics [28], and the effect of down regulation [29], the values of N_A and N_B are governed by the equilibrium constant as follows:

$$\frac{K(T_A)}{c} = \left(\frac{0.5N_0 - N_A}{N_A}\right)$$
$$\frac{K(T_B)}{c} = \left(\frac{0.5N_0 - N_B}{N_B}\right) \quad (6)$$

where K is the equilibrium constant of the ligand–receptor interaction and T_A and T_B denote the temperatures on side A and B respectively. The equilibrium constant K of biochemical reactions generally exhibits Arrhenius-type temperature dependence. As a result, a large enough temperature difference between A and B may result in a significant difference $N_A - N_B$ given below:

$$\Delta N = N_A - N_B = 0.5N_0 \left[\frac{1}{1 + K(T_A)/c} - \frac{1}{1 + K(T_B)/c}\right] \quad (7)$$

Eq. (7) may be non-dimensionalized as follows:

$$\Delta f = f_A - f_B = \left[\frac{1}{1 + K(T_A)/c} - \frac{1}{1 + K(T_B)/c}\right] \quad (8)$$

where f is the fractional site occupancy, obtained by dividing the number of occupied sites with the total number of sites on each side of the cell. Δf refers to the difference in the fractional site occupancy between the two sides of the cell.

Assuming that the temperature difference $T_A - T_B$ is small, one may linearize to write

$$K(T_B) = K(T_A) + \frac{dK}{dT}\Delta T \quad (9)$$

or,

$$\frac{K(T_B)}{K(T_A)} = 1 + \frac{1}{K}\frac{dK}{dT}\Delta T = 1 + \alpha_K \Delta T \quad (10)$$

α_K is the temperature coefficient of the equilibrium constant and indicates how strongly dependent on temperature K is.

Substituting from Eq. (10) in Eq. (8), one may derive an expression of the difference in the fractional site occupancy across the cell as a function of the temperature difference, the temperature coefficient of equilibrium constant and the non-dimensional ligand concentration.

$$\Delta f = \frac{(K/c)\alpha_K \Delta T}{(1 + K/c)(1 + (K/c)(1 + \alpha_K \Delta T))} \quad (11)$$

As with chemotaxis, a cell response is triggered when this difference in fractional occupancy across the cell exceeds a certain threshold value denoted by Δf^*. The condition for thermotaxis may thus be written as

$$\frac{(K/c)\alpha_K \Delta T}{(1 + K/c)(1 + (K/c)(1 + \alpha_K \Delta T))} > \Delta f* \quad (12)$$

The value of Δf^* has been established to be around 0.5–2% across a typical cell [24,30–32]. Studies involving a wide variety of cell types including nerve cells, fibroblasts and unicellular organisms agree remarkably well with each other for the value of this threshold chemical gradient, suggesting that the ligand-binding interactions are a fundamental cellular sensory process across different species.

The predictions of this theoretical model are discussed in Section 4.2.

4. Results and discussion

4.1. Thermal characterization of microheater device

The temperature sensors on the microheater platform are first calibrated by measuring their electrical resistance at different temperatures in a constant-temperature chamber. As expected, calibration curves are very nearly linear in the temperature range of interest. Based on the calibration curves, Fig. 5 plots the heater temperature rise as a function of heating power and compares experimental data with the model prediction. There is excellent agreement between the two. Comparison of experimental data with the slope predicted by Eq. (5) provides the thermal conductivity of the membrane material, a key parameter required for detailed temperature prediction on the membrane during experiments with cells. The thermal conductivity of the silicon nitride based membrane is found to be 0.52 W/mK, which agrees well with previously reported data on this material [14,15].

Fig. 6 shows a representative temperature profile on the microheater platform determined using finite element simulations. Note

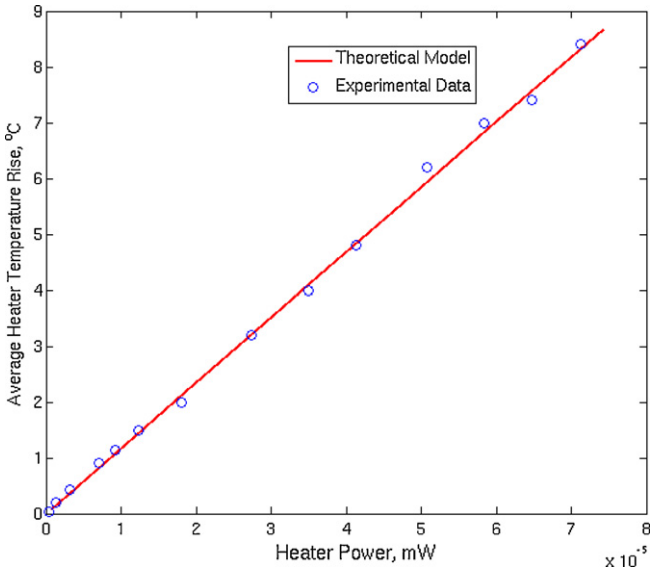

Fig. 5. Experimental data for heater temperature rise as a function of power compared with analytical model, Eq. (5).

the curvature in the temperature field around the temperature sensor elements. This is due to heat conduction down the metal wires leading to the sensors. Finite element simulation enables the determination of temperature and the thermal gradient experienced by a cell adhered to a given location on the microheater platform.

4.2. Theoretical and experimental results for thermotaxis

The microheater platform is first used to demonstrate the effect of temperature on cell viability. The viability of cells cultured on the microheater device is expected to depend on the local temperature experienced by them in the temperature field generated by the microheater device. Varying magnitudes of heating current are passed through the metal heater in different microdevices in order to study this effect. When the heating current is small, typically tens of μA, the temperature rise is small, and as a result, no effect on cell viability is expected. Figs. 7(a)–(d) show fluorescent images of cells after 6 h of exposure to Joule heating by 10 μA, 100 μA, 700 μA and 1.0 mA electric current respectively. The corresponding maximum temperature rise for these electric currents are 0.04 °C, 0.4 °C, 20 °C and 40 °C respectively. The heater line, not shown in these

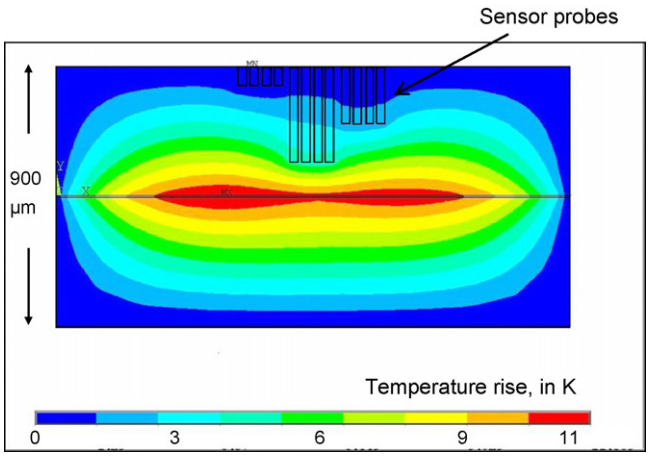

Fig. 6. FEM simulation for the temperature field on the microheater platform. Note the curvature in the field around the sensor probes, due to heat conduction down the sensor wires.

figures, is located beyond the bottom-left corner of the image. As expected, the mild heating caused in the first two cases has no influence on cells, which continue to adhere well and remain viable on the microheater surface, as shown in Fig. 7(a) and (b). On the other hand, a larger heating current causes cell death, particularly for cells located close to the metal heater. In each case, the maximum temperature exists next to the heater line, and the temperature falls off as the distance from the heater increases. Cells cultured close to the heater are seen to lose viability due to exposure to the large temperature rise. On the other hand, cells far away from the heater do not experience such a severe impact and continue to remain viable. There is an intermediate region where some cells are alive and others are dead. The approximate location of the live–dead boundary may be controlled by changing the heater current. The larger the heating current, the farther would the influence of the thermal field on cultured cells extend. In the case of a very large heating current, buoyancy-driven flow is also observed within the chamber defined by the PDMS gasket. This flow is capable of moving cells suspended in the media. It may be possible to engineer precise motion of cells based on buoyancy-driven flow by careful design of the chamber. However, this effect was not studied in detail since the temperature rise required for such motion is likely to be too large to simultaneously keep cells viable.

The ability to selectively control cell viability at the scale of tens of microns demonstrated through the microheater device has several interesting applications. Temperature control at the microscale may be useful as a tool for spatially selective lysing for a variety of detection assays. Precise control of temperature of a thin film surface may also be useful for control and manipulation of biological macromolecules like DNA, proteins, etc.

Experiments aimed at observing thermotactic effects on individual cells are carried out next. The primary goal of these experiments is to explore whether cells exhibit chemotaxis-like behavior in response to an imposed temperature gradient. This is of much theoretical interest since thermotactic behavior is well known at the organismal level, but not much work exists on this phenomenon at the cellular level [12,13]. While all constituent cells may not exhibit organismal level behavior due to specialization, very little is known about which mammalian cells may exhibit thermotactic behavior. As a result, the choice of cells for this experiment is not straightforward. The theoretical model for thermotaxis presented in the next section links thermotaxis to chemotactic activity. As a result, PC12 and 3T3 cells are chosen for this work, since these cells are well known for exhibiting chemotactic activity [19,20]. Cells adhered to the microheater membrane are subjected to varying magnitudes of temperature gradients, ranging between 0.1 °C and 10 °C across a cell with an approximate dimension of 15 μm. Experimental times range from a few seconds to as long as several hours. Experiments with PC12 cells are carried out both with and without nerve growth factor (NGF), which is a well known neurotrophin for the PC12 cell line [19]. None of the temperature gradients and exposure times in the experimental matrix elicited any thermotactic response from cells. An extremely large temperature gradient is found to cause cell death, just as expected. The lack of thermotactic activity is observed both when the ambient is at room temperature as well as at 37 °C. In another version of the microheater device, two heater lines were used instead of one (Fig. 8), enabling independent temperature control on either side of the cell. Cells adhered to the microheater surface between the two heater lines also failed to exhibit any thermotactic response in this case.

In order to better understand the experimental result, the theoretical response of a cell to a temperature gradient as predicted by the theoretical model presented in Section 3.2 is examined. Figs. 9(a) and (b) plot Δf as a function of the imposed temperature gradient for two values of equilibrium constant and α_K respectively. By comparing Δf to Δf^*, the threshold temperature gradient may

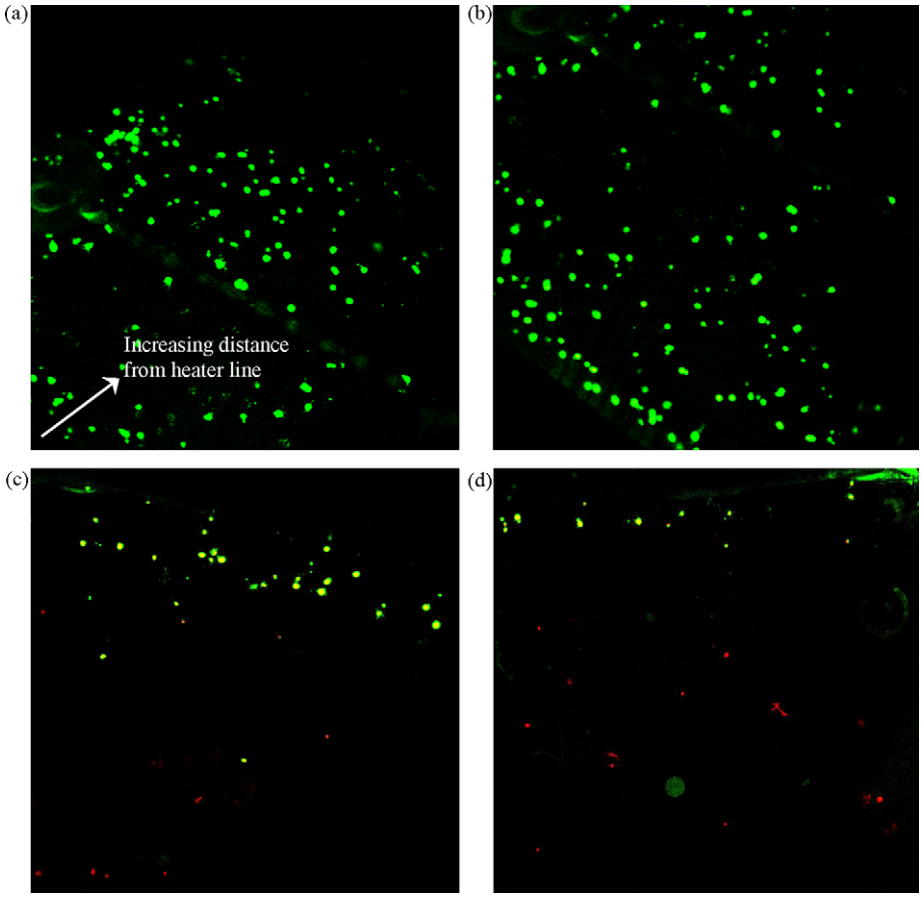

Fig. 7. Fluorescent images of PC12 cells subjected to (a) 10 μA, (b) 100 μA, (c) 700 μA and (d) 1 mA heating current. Green and red colors indicate viable and unviable cells respectively. (For interpretation of the references to color in the citation of this figure, the reader is referred to the web version of the article.)

be determined. Fig. 9(a) and (b) shows that ΔT^* is a strong function of both K and α_K. The value of α_K – which represents the temperature dependence of K – is not well known for most ligand-binding interactions of interest. Limited studies have measured the reaction rates of these interactions at specific temperatures. Equilibrium constants for PC12–NGF and NB–NGF binding have been measured at 37 °C and 4 °C respectively [28,33]. By assuming an Arrhenius-type temperature dependence of α_K, the value of α_K in both cases is found to be around 4.26% °C^{-1}. Aside from these two interactions, data for α_K are very scarce. The uncertainty over the value of α_K makes thermotaxis difficult to predict and observe in experiments. Another important reason behind the difficulty of experimental observation of thermotaxis is the narrow temperature window in which most cells survive. Most mammalian cells survive within a 5–10 °C temperature range above their normal temperature. If ΔT^* is greater than this range, cells will begin to lose viability due to the increase in absolute temperature caused by the temperature gradient. This could be the fundamental reason why chemotaxis, and not thermotaxis is the primary mechanism behind several cellular processes.

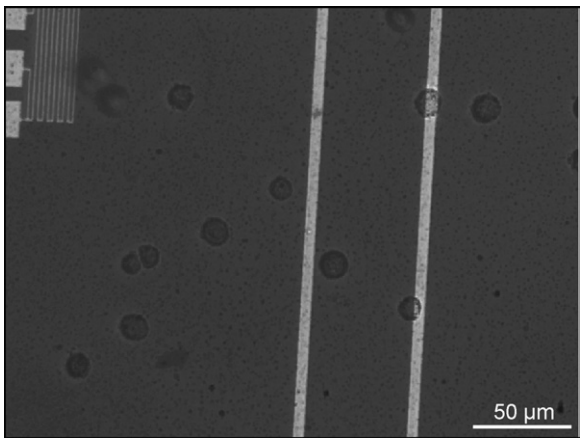

Fig. 8. Image of the two-heater microheater platform. Presence of two heaters enables independent control of temperature on either ends of a cell adhered between the heaters.

In addition to throwing light on parameters influencing cellular thermotaxis, the theoretical model may also explain the well known correlation between chemical and thermal gradients [34]. By considering simultaneous thermal and chemical gradients applied across a cell, one may derive the following equation that incorporates the effects of both thermal and chemical gradients on the fractional difference in receptor occupancy.

$$\Delta f = \left[\frac{(K/c)(\alpha_k \Delta T - \alpha_c \Delta x)}{(1 + K/c)(1 + (K/c)(1 + \alpha_k \Delta T) + \alpha_c \Delta x)}\right] \quad (13)$$

where Δx is the cell size and α_c is the gradient of chemical species, such that $c_B = c_A(1 + \alpha_c \Delta x)$.

Eq. (13) explains the experimental evidence [33] that thermal and chemical stimuli may complement or cancel each others' effect depending on the direction of application. Depending on the signs of α_K and α_c, the effects of thermal and chemical stimuli on Δf may be either complementary or opposite. Fig. 10 plots the temperature and chemical gradients applied across a cell and shows a curve of the threshold ligand-binding difference. All temperature and chemical gradient combinations beneath the curve are insuf-

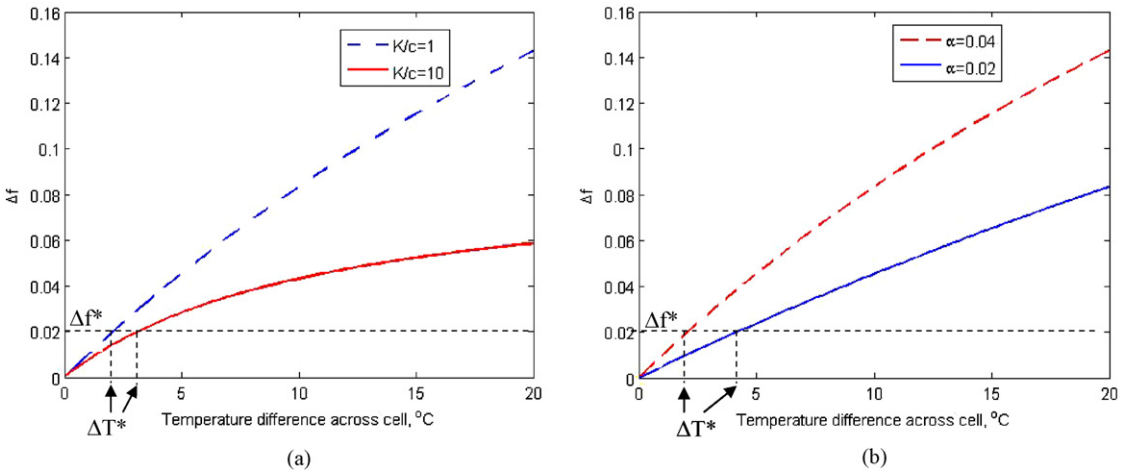

Fig. 9. Plot of the difference in fractional occupancy, Δf as a function of the temperature difference across the cell, for two different values of (a) equilibrium constant, K, and (b) α_K, temperature coefficient of K. Note the strong dependence of Δf^* and ΔT^* on both K and α_K. A temperature gradient greater than around 5 °C is infeasible due to the large absolute temperature.

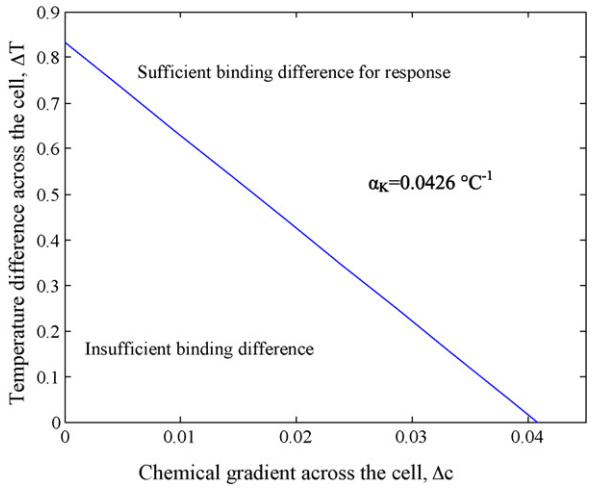

Fig. 10. A plot of imposed chemical and temperature gradients across a cell, showing the curve of sufficient ligand-binding difference. Any thermal–chemical combination above the curve is sufficient to induce cell response. This plot shows the synergistic manner in which chemical and thermal gradients may combine with each other.

ficient to induce cell response. Increasing any or both of them in order to cross the curve will result in cell response. The x and y intercepts of the curve in Fig. 10 represent the chemical and temperature gradients needed to induce cell response independently in the absence of each other.

5. Conclusion

This paper discusses the design and microfabrication of a microheater platform capable of generating thermal signals at the same spatial scale as typical cells. The MEMS-based microheater platform demonstrates the capability of microscale experimental tools to overcome the traditional inability of experimental tools to manipulate temperature at the same scale as typical cells. The capabilities of the microheater platform may be applicable in a variety of experiments involving the interaction of biological microsystems with their thermal microenvironment. For example, the spatial control of cell lysing using temperature as a tool is quite promising. Further, it may be possible to re-engineer the microheater platform to provide measurable temporal thermal gradients in addition to spatial gradient. The theoretical model for thermotaxis presented in this paper throws light on the fundamental biophysics of thermal sensing in a cell and suggests a close association between thermal and chemical gradient sensing. The model predicts that cells may sense temperature gradient using the same mechanism used for sensing chemical gradients, and that beyond a threshold value, the temperature gradient may cause thermotactic response similar to chemotactic response. The accuracy of the model predictions is limited by the lack of data for temperature dependent equilibrium constants for ligand–receptor interactions. The model suggests that the lack of experimental observation of thermotaxis may be due to the fact the threshold gradient needed for thermotaxis may be too high, resulting in the absolute temperature exceeding the temperature limit for cell survival. The model suggests that this could be the fundamental reason behind the dominance of chemical gradients over thermal gradients for regulating cellular activity.

Acknowledgments

Financial support from the Stanford Graduate Fellowships (SGF) is gratefully acknowledged. Microfabrication of the devices described in this paper was carried out at the Stanford Nanofabrication Facility (SNF). The authors would like to acknowledge Dr. Harvey Fishman, Neville Mehenti, Mark Peterman, Prof. Beth Pruitt and Vikram Mukundan for their assistance with cell culturing.

References

[1] D.L. Polla, A.G. Erdman, W.P. Robbins, D.T. Markus, J. Diaz-Diaz, R. Rizq, Y. Nam, H.T. Brickner, A. Wang, P. Krulevitch, Microdevices in medicine, Annu. Rev. Biomed. Eng. 2 (2000) 551–576.
[2] K. Petersen, Biomedical applications of MEMS, in: Technical Digest—International Electron Devices Meeting, 1996, pp. 239–242.
[3] A. van den Berg, T.S.J. Lammerink, Micro total analysis systems: microfluidic aspects, integration concept and applications, Top. Curr. Chem. 194 (1998) 21–49.
[4] Y.-C. Lin, M.-Y. Huang, K.-C. Young, T.-T. Chang, C.-T. Wu, A rapid micro polymerase chain reaction system for hepatitis C virus amplification, Sens. Actuators B 71 (2000) 2–8.
[5] P. Belgrader, W. Benett, D. Hadley, J. Richards, P. Stratton, R. Mariella Jr., F. Milanovich, PCR detection of bacteria in seven minutes, Science 284 (2000) 449–450.
[6] D. Ross, L.E. Locascio, Microfluidic temperature gradient focusing, Anal. Chem. 74 (2002) 2556–2564.
[7] D.J. Sadler, R. Changrani, P. Roberts, C. Chou, F. Zenhausern, Thermal management of BioMEMS, Proc. Intersoc. Conf. Therm. Phenom. (2002) 1025–1032.
[8] A. Folch, M. Toner, Microengineering of cellular interactions, Annu. Rev. Biomed. Eng. 2 (2000) 227–256.
[9] A. Kuhara, M. Okumura, T. Kimata, Y. Tanizawa, R. Takano, K.D. Kimura, H. Inada, K. Matsumoto, I. Mori, Temperature sensing by an olfactory neuron in a circuit controlling behavior of *C. elegans*, Science 320 (2008) 803–807.

[10] F.U. Hartl, W. Neupert, Protein sorting to mitochondria: evolutionary conservations of folding and assembly, Science 23 (1990) 930–938.
[11] R.M. Wartell, S. Hosseini, S. Powell, J. Zhu, Detecting single base substitutions, mismatches and bulges in DNA by temperature gradient gel electrophoresis and related methods, J. Chromatogr. A 806 (1998) 169–185.
[12] W.S. Ryu, A.D. Samuel, Thermotaxis in *Caenorhabditis elegans* analyzed by measuring responses to defined thermal stimuli, J. Neurosci. 22 (2002) 5727–5733.
[13] E. Hedgecock, R. Russell, Normal and mutant thermotaxis in the nematode *Caenorhabditis elegans*, Proc. Natl. Acad. Sci. U.S.A. 72 (1975) 4061–4065.
[14] D. Briand, S. Heimgartner, M. Gretillat, B. van der Schoot, N.F. de Rooij, Thermal optimization of micro-hotplates that have a silicon island, J. Micromech. Microeng. 12 (2002) 971–978.
[15] H.C. Berg, E.M. Purcell, Physics of chemoreception, Biophys. J. 20 (1977) 193–219.
[16] I. Mori, Y. Ohshima, Neural regulation of thermotaxis in *Caenorhabditis elegans*, Nature 376 (1995) 344–348.
[17] K. Venkatachalam, C. Montell, TRP channels, Annu. Rev. Biochem. 76 (2007) 387–417.
[18] A. Dhaka, V. Viswanath, A. Patapoutian, TRP ion channels and temperature sensation, Annu. Rev. Neurosci. 29 (2006) 135–161.
[19] L.A. Greene, A.S. Tischler, Establishment of noradrenergic clonal line of rat adrenal Pheochromocytoma cells which respond to nerve growth factor, Proc. Nat. Acad. Sci. U.S.A. 73 (1976) 2424–2428.
[20] G.J. Todaro, H. Green, Quantitative studies of the growth of mouse embryo cells in culture and their development into established lines, J. Cell Biol. 17 (1963) 299–313.
[21] http://probes.invitrogen.com/media/pis/mp03224.pdf (accessed August 08, 2009).
[22] K.E. Goodson, Y.S. Ju, Heat conduction in novel electronic films, Annu. Rev. Mater. Res. 29 (1999) 261–293.
[23] X. Zhang, C.P. Grigoropoulos, Thermal conductivity and diffusivity of free-standing silicon nitride thin films, Rev. Sci. Instrum. 66 (1995) 1115–1120.
[24] B.K. Mueller, Growth cone guidance: first steps towards a deeper understanding, Annu. Rev. Neurosci. 22 (1995) 351–388.
[25] C.E. Schmidt, J.B. Leach, Neural tissue engineering: strategies for repair and regeneration, Annu. Rev. Biomed. Eng. 5 (2003) 293–347.
[26] S.R. Cajal, Degeneration and Regeneration of The Nervous System, Oxford University Press, London, 1928, translator R.M. May.
[27] G.J. Goodhill, J.S. Urbach, Theoretical analysis of gradient detection by growth cones, J. Neurobiol. 41 (1999) 230–241.
[28] A.L. Schechter, M.A. Bothwell, Nerve growth factor receptors on PC12 cells: evidence for two receptor classes with differing cytoskeletal association, Cell 24 (1981) 867–874.
[29] S.J. Sullivan, S.H. Zigmond, Chemotactic peptide receptor modulation in polymorphonuclear leukocytes, J. Cell. Biol. 85 (1980) 703–711.
[30] H. Baier, F. Bonhoeffer, Axon guidance by gradients of a target-derived component, Science 255 (1991) 472–475.
[31] J.M. Mato, A. Losada, V. Nanjundiah, T. Konjin, Signal input for a chemotactic response in the cellular slime mold *Dictyostelium discoideum*, Proc. Nat. Acad. Sci. U.S.A. 72 (1975) 4991–4993.
[32] G.R. Lewin, Y.A. Barde, Physiology of the neurotrophins, Annu. Rev. Neurosci. 19 (1996) 289–317.
[33] K. Sonnenfeld, D.N. Ishii, Fast and slow nerve growth factor binding sites in human neuroblastoma and rat PC12 cell lines: relationship of sites to each other and to neurite formation, J. Neurosci. 5 (1985) 1717–1728.
[34] J.O. Kessler, L.F. Jarvik, T.K. Fu, S.S. Matsuyama, Thermotaxis, chemotaxis and age, Age 2 (1979) 5–11.

Biographies

Ankur Jain received his Ph.D. (2007) and M.S. (2003) in mechanical engineering from Stanford University and B.Tech. (2001) in mechanical engineering from the Indian Institute of Technology (IIT), Delhi. At present, Ankur is a Sr. Research Engineer at Molecular Imprints, Inc. at Austin, TX, USA. His research interests include Bio-MEMS, biophysics, thermal phenomena in biological microsystems, microscale heat transfer, etc.

Kevin Ness received his Ph.D. (2006) in mechanical engineering from Stanford University. He currently works at Quanta Life Inc. at Livermore, CA, USA. His research interests include Bio-MEMS, microfluidics, etc.

Kenneth Goodson is Professor and Vice Chair of Mechanical Engineering at Stanford University. Goodson was educated at MIT (Ph.D. 1993, M.S. 1991, BSME 1989, BSH 1989) and spent two post-doctoral years with the Materials Group at Daimler-Benz AG. His Stanford research group includes approximately 20 students, research associates, and affiliated faculty. The group studies thermal transport phenomena in semiconductor nanostructures, energy conversion devices, and microfluidic heat sinks, with a focus on those occurring with very small length and time scales. Goodson is a co-founder and former CTO of Cooligy, Inc., which builds microfluidic cooling systems for computers and was acquired by Emerson, Inc., in 2005. Goodson received the ASME Journal of Heat Transfer Outstanding Reviewer Award, and now serves as an Associate Editor for this journal. Goodson serves as Editor-in-Chief of Nanoscale and Microscale Thermophysical Engineering. He has been a JSPS Visiting Professor at The Tokyo Institute of Technology and received the ONR Young Investigator Award and the NSF CAREER Award. He and his group have published more than 100 archival journal articles, 150 conference papers, and ten books and book chapters, which have been recognized through best paper awards at SEMI-THERM, the Multilevel Interconnect Symposium, SRC TECHCON, and the IEDM.